



**HAL**  
open science

## A 3D approach to model the taper of irregular tree stems: making plots biomass estimates comparable in tropical forests

Sebastien Bauwens, Pierre Ploton, Adeline Fayolle, Gauthier Ligot, Jean Joël Loumeto, Philippe Lejeune, Sylvie Gourlet-Fleury

### ► To cite this version:

Sebastien Bauwens, Pierre Ploton, Adeline Fayolle, Gauthier Ligot, Jean Joël Loumeto, et al.. A 3D approach to model the taper of irregular tree stems: making plots biomass estimates comparable in tropical forests. *Ecological Applications*, 2021, 31 (8), 10.1002/eap.2451 . hal-03470860

**HAL Id: hal-03470860**

**<https://hal.inrae.fr/hal-03470860>**

Submitted on 20 Jul 2023

**HAL** is a multi-disciplinary open access archive for the deposit and dissemination of scientific research documents, whether they are published or not. The documents may come from teaching and research institutions in France or abroad, or from public or private research centers.

L'archive ouverte pluridisciplinaire **HAL**, est destinée au dépôt et à la diffusion de documents scientifiques de niveau recherche, publiés ou non, émanant des établissements d'enseignement et de recherche français ou étrangers, des laboratoires publics ou privés.



Distributed under a Creative Commons Attribution - NonCommercial - NoDerivatives 4.0 International License

DR. GAUTHIER LIGOT (Orcid ID : 0000-0002-5508-4358)

Article type : Article

Journal: Ecological Applications

Manuscript type: Articles

**Running Head:** 3D taper and tropical forest biomass

**A 3D approach to model the taper of irregular tree stems: making plots biomass estimates comparable in tropical forests**

S. Bauwens<sup>1,6</sup>, P. Ploton<sup>2</sup>, A. Fayolle<sup>1</sup>, G. Ligot<sup>1</sup>, J. J. Loumeto<sup>3</sup>, P. Lejeune<sup>1</sup>, and S. Gourlet-Fleury<sup>4,5</sup>

1. TERRA Teaching and Research Centre - Forest is Life, Gembloux Agro-Bio Tech, University of Liege, 5030 Gembloux, Belgium

2. AMAP, Univ Montpellier, IRD, CNRS, INRAE, CIRAD, Montpellier, France

3. University Marien NGOUABI. Faculté des Sciences et Techniques. Laboratoire de Botanique et Écologie. B.P. 69. Brazzaville, Republic of Congo.

4. CIRAD, Forêts et Sociétés, F-34398 Montpellier, France.103.

5. Forêts et Sociétés, Univ Montpellier, CIRAD, Montpellier, France.

6. Corresponding author. E-mail: Bauwens.sebastien@gmail.com

This article has been accepted for publication and undergone full peer review but has not been through the copyediting, typesetting, pagination and proofreading process, which may lead to differences between this version and the [Version of Record](#). Please cite this article as [doi: 10.1002/EAP.2451](#)

This article is protected by copyright. All rights reserved

Manuscript received 11 December 2020; revised 11 March 2021; accepted 6 April 2021; final version received 31 August 2021.

Accepted Article

## ABSTRACT

In tropical forests, the high proportion of trees showing irregularities at the stem base complicates forest monitoring. For example, in the presence of buttresses, the height of the point of measurement ( $H_{\text{POM}}$ ) of the stem diameter ( $D_{\text{POM}}$ ) is raised from 1.3 m, the standard breast height, up to a regular part of the stem. While  $D_{\text{POM}}$  is the most important predictor for tree aboveground biomass (AGB) estimates, the lack of harmonized  $H_{\text{POM}}$  for irregular trees in forest inventory increases the uncertainty in plot-level AGB stock and stock change estimates. In this study, we gathered an original non-destructive 3D dataset collected with terrestrial laser scanning and close range terrestrial photogrammetry tools in three sites in central Africa. For the 228 irregularly shaped stems sampled, we developed a set of taper models to harmonize  $H_{\text{POM}}$  by predicting the equivalent diameter at breast height (DBH') from a  $D_{\text{POM}}$  measured at any height. We analyzed the effect of using DBH' on tree-level and plot-level AGB estimates. To do so, we used destructive AGB data for 140 trees and forest inventory data from eight 1-ha-plots in the Republic of Congo. Our results showed that our best simple taper model predicts DBH' with a relative mean absolute error of 3.7% ( $R^2=0.98$ ) over a wide  $D_{\text{POM}}$  range of 17 to 249 cm. Based on destructive AGB data, we found that the AGB allometric model calibrated with harmonized  $H_{\text{POM}}$  data was more accurate than the conventional local and pantropical models. At the plot level, the comparison of AGB stock estimates with and without  $H_{\text{POM}}$  harmonization showed an increasing divergence with the increasing share of irregular stems (up to -15%). The harmonization procedure developed in this study could be implemented as a standard practice for AGB monitoring in tropical forests as no additional forest inventory measurements is required. This would probably lead to important revisions of the AGB stock estimates in regions having a large number of irregular tree stems and increase their carbon sink estimates. The growing use of 3D data offers new opportunities to extend our approach and further develop general taper models in other tropical regions.

**Key-words:** 1) Allometric above-ground biomass model, 2) biomass changes, 3) buttresses, 4) close-range terrestrial photogrammetry, 5) point of measurement of stem diameter, 6) stem profile 7) taper, 8) terrestrial laser scanning, 9) structure from motion

# 1 Introduction

Tropical forests play a key role in the terrestrial global carbon cycle (Pan et al., 2011), but their estimated contribution and response to global environmental changes are still subject to a high degree of uncertainty (Mitchard et al., 2014, 2013; Phillips and Lewis, 2014).

Estimates of forest carbon stocks are mainly based on indirect tree-level biomass estimates, using allometric models to convert forest inventory data into aboveground biomass (AGB, Fig. 1). Tree biomass estimates are then summed at the plot scale and the resulting plots biomass estimates are then upscaled to larger areas (e.g., a landscape, a region, a country) using design- or model-based inference approaches, with or without ancillary data (McRoberts, 2010; McRoberts et al., 2010, Clark and Kellner, 2012; Gibbs et al., 2007).

It has been demonstrated that the propagation of errors from tree measurements to large-scale carbon stock estimates largely depends on the choice of the AGB allometric model (Chave et al., 2004; Chen et al., 2016; Molto et al., 2013; Zhao et al., 2012). In the tropics, general (multi-species) AGB models are most commonly used to predict tree AGB (Brown et al., 1989; Chave et al., 2014, 2005; Fayolle et al., 2018, 2013; Higuchi et al., 1998; Nogueira et al., 2008; Overman et al., 1994). General allometric models typically use tree diameter ( $D_{\text{POM}}$ ) measured at the point of measurement (POM), which is either the 1.3 m reference height or above any deformation, total tree height (TH) and species average wood basic density ( $\rho$ ) as predictors.

When developing AGB models, an important step of model diagnosis consists of assessing how model error varies with change in fitted or predictor values. The pantropical AGB model of Chave et al. (2014), which is the most widely used model, shows a clear error pattern with tree biomass, with a large AGB overestimation for small trees and an underestimation for large trees ( $> 20$  Mg, Fig. 2 in Chave et al. 2014). Using the publicly available dataset of Chave et al. (2014), it can be shown that the error shows a similar structure with tree diameter, with a positive mean relative error for trees with diameter  $\leq 140$  cm (mean = 14%, median = 7 % and  $n = 3,988$ ) and, a negative mean relative error for the trees larger than 140 cm (mean = -14 %, median = -16 %,  $n = 16$  and a maximum diameter of 212 cm). This systematic underestimation of AGB for large trees has been found in independent studies using this pantropical model or a similar AGB model functional form (*i.e.*, a power model based on the compound variable  $\rho \cdot D_{\text{POM}}^2 \cdot \text{TH}$ ) in Amazonia (Gonzalez de Tanago et al., 2018; Goodman et al., 2014; Lau et al., 2019) and central Africa (Bauwens et al.,

2017; Ploton et al., 2016). A hypothesis to explain this bias is that variation in crown-diameter allometry, either across sampling sites (Goodman et al., 2014) or during tree ontogeny (Ploton et al., 2016), is not fully captured by the model's predictors (i.e.,  $D_{POM}$ , TH and  $\rho$ ) while it influences tree allometry. Another hypothesis for the underestimation of large tree AGB is that such trees often present deformations (e.g., buttresses) at the standard breast height (i.e., 1.3 m) so that the measured diameter ( $D_{POM}$ ) is taken higher and is systematically lower than the equivalent diameter at breast height because of stem taper. Bauwens et al. (2017) developed a method based on 3D data to harmonize the height ( $H_{POM}$ ) of the measured  $D_{POM}$  by computing the equivalent diameter at breast height (DBH') which is defined as the diameter of a circle having the same area as the measured basal area at 1.3 m height. Using destructive biomass data from Cameroon, the authors demonstrated that using DBH' instead of  $D_{POM}$  in a published AGB model reduced the AGB underestimation for large trees with an irregular stem (Fig. 4 in Bauwens et al. 2017). This last method has operational perspectives as DBH' could be estimated from correction models previously fitted on 3D data without requiring additional measurements in forest inventories.

Across 97 1-ha forest inventory plots in central Africa (from a subsample of Ploton et al., 2020),  $H_{POM}$  values greater than 1.3 m represent 9% ( $\pm 9\%$ ) of the trees with  $D_{POM} \leq 70$  cm and this proportion rises to 55% ( $\pm 31\%$ ) for trees with  $D_{POM} > 70$  cm, suggesting that trees with irregular stem base dominate among large tropical trees in this region. Since large trees disproportionately contribute to AGB stocks (Bastin et al., 2015; Lutz et al., 2012; Slik et al., 2013), any systematic errors in AGB prediction induced by the use of non-standard  $H_{POM}$  would have an important influence on plot AGB estimates and associated uncertainties (Cushman et al., 2014; Muller-Landau et al., 2014). The influence of this error pattern on the changes of the biomass stock over time is less easy to apprehend since biomass production is not driven by large trees (Ligot et al., 2018). Therefore, it remains unclear how the abundance of trees with irregular stem bases could affect estimates of stand biomass productivity and carbon capture. In all cases, the conversion of  $D_{POM}$  to DBH' whether using taper models (Bauwens et al., 2017; Cushman et al., 2014) or empirical statistical models (Bauwens et al., 2017; Ngomanda et al., 2012), has the potential to improve plot AGB estimates and their comparison (among plots and over time). The use of a taper model compared to empirical statistical models has the advantage to be less sensitive to field protocol for measuring the diameter of trees with irregularities at the standard height (e.g. of field protocols:  $D_{POM}$  measured 30 or 50 cm, 1 m or even more above the buttresses).

In this study, we developed a correction procedure aiming to harmonize the  $H_{\text{POM}}$  by estimating  $\text{DBH}'$ , the equivalent diameter at the standard breast height (1.3 m), for irregular tree stems and assess its effect on biomass estimates at the tree and plot level. Specifically, we (i) used 3D tree data to develop a general taper model that predicts  $\text{DBH}'$  from information available in conventional forest inventories. Then we (ii) used destructive AGB data to assess the potential fit improvement in allometric models by using  $\text{DBH}'$  in the AGB predictors instead of  $D_{\text{POM}}$ . We also assessed the prediction error of the pantropical AGB model when using  $\text{DBH}'$  instead of  $D_{\text{POM}}$  in the model. Last, we (iii) used forest inventory data to evaluate the effect of the  $H_{\text{POM}}$  harmonization on biomass stocks and stock changes at the plot level, considering our local AGB model fitted with  $\text{DBH}'$  as the reference.

## 2 Material and methods

### 2.1 The taper study sites

We collected 3D data on 228 trees, distributed in three sites in central Africa. A total of 40 trees were sampled in the first site in Cameroon ( $14^{\circ}6.867'$  N,  $14^{\circ}33.133'$  E) using terrestrial laser scanning (TLS), 102 trees were sampled in the second site in the Republic of Congo ( $2^{\circ}22.520'$  N,  $17^{\circ}4.771'$  E) using close range terrestrial photogrammetry (CRTP), and 86 trees were sampled in the third site in the Democratic Republic of Congo ( $0^{\circ}12.057'$  N,  $25^{\circ}20.580'$  E) using TLS (Appendix S1: Table S1). We recorded the tree species, the  $H_{\text{POM}}$  and the  $D_{\text{POM}}$  of each sampled tree.  $H_{\text{POM}}$  was measured using a laser rangefinder device (VERTEX IV) and,  $D_{\text{POM}}$  was measured with a tape or, if the height of measurement was too high ( $H_{\text{POM}} > 4.5$  m), in the lab by automatically extracting  $D_{\text{POM}}$  at the required measured  $H_{\text{POM}}$  with the 3D data from TLS or CRTP. Before collecting 3D data of the trees, we cleared the small vegetation (stem with diameter  $< 5$  cm and leaves) and small lianas up to 2 m high in a radius  $< 2.5$  m around the focal trees.

We selected eleven abundant focal species with potential stem irregularities and for each of them, we sampled at least five trees spanning a diameter range as wide as possible. To expand our analysis to a large variety of stem shapes, we also selected less abundant species with contrasted stem irregularities and species with more regular stems. For the analyses, we defined a categorical variable called 'Species' that separately includes the focal species, two other species with more than five trees measured and having contrasted shapes (Emien - *Alstonia boonei* De Wild with its

potential fluted trunk and Iroko - *Milicia excelsa* (Welw.) C.C. Berg with its more regular shape) and a group gathering the species with less than five trees (totaling 32 trees). The variable 'Species' thus contains 14 categories (eleven focal species, two other species with more than five trees, one group of other species with 31 trees, Appendix S1: Table S1).

## 2.2 Post-processing of 3D point clouds

We extracted trunk metrics of the 3D point clouds obtained from TLS and CRTP by following the workflow detailed in Bauwens et al. (2017). The outputs are cross-sections realized every 10 cm along the stem axis up to 1 meter above the  $H_{POM}$  of each tree. For each cross-section (Fig. 2), we extracted: (i) diameter of a theoretical circle which area equals the real area of the cross-section at that height  $l$  ( $D_{area,l}$ , in meter), (ii) the convex hull length that imitates a tape tight around the stem, express in equivalent diameter ( $D_{convHull,l}$ , in meter) and, (iii) the perimeter expressed in equivalent diameter of a circle with the same perimeter ( $D_{perim,l}$ , in meter).

## 2.3 Taper profiles of irregularly shaped tree stems

Most taper models require total tree height to express height in relative terms. Tree height is, however, difficult to measure in tropical forests and subject to large measurement uncertainties due to a frequently high, dense, and multi-layered canopy. This variable, hence, is not systematically available in forest inventory datasets. We therefore tested a variety of taper models (Appendix S1: Table S2) that does not require total tree height as an explicative variable and which rely on few parameters to ease further analyses. Based on the best Akaike Information Criterion ( $AIC = 2k - 2\ln(L)$ ), the Root Mean Square Error ( $RMSE = \sqrt{\frac{1}{n} \cdot \sum_1^n (\hat{D}_{area,l,k} - D_{area,l,k})^2}$ ) and the simplicity of the model, we finally selected the following model:

$$D_{area,l} = \frac{D_{POM} h_l^\alpha}{H_{POM}^\alpha} + \varepsilon_l \quad 2.$$

With,  $D_{area,l}$ : the equivalent diameter of the cross-section area  $l$  at the height  $h_l$  (in meter),  $D_{POM}$ : the diameter measured in the field (50 cm above the buttresses or above other local deformations; in meter),  $h_l$ : the height  $l$  above the ground and along the stem at which  $D_{area,l}$  is predicted (in meter),  $H_{POM}$ : the height of measurement of  $D_{POM}$  (in meter) and,  $\alpha$ : the taper parameter.

## 2.4 Prediction of the taper parameter

After identifying the taper model that fits the best at the tree-level, we generalized Eq. 2. to predict the most reliable equivalent diameter (DBH') for any tree measured in forest inventories (Eq. 3.).

We used different covariates that would potentially explain individual variations of the taper parameter  $a_{i,j,k}$ . These covariates are the species and the site (both categorical covariates) and quantitative trunk metrics based on measured (or easily measurable) variables in forest inventories:  $D_{POM}$ ,  $H_{POM}$ ,  $D_{convhull130}$ , buttresses convex taper –  $bct$ , slenderness coefficients –  $h:d$ ,  $h:d^2$ ,  $h:d_c$ ,  $h:d_c^2$ , hardness coefficient –  $hdn$  and the deficit basal area index –  $DeBA$  (definitions in Appendix S1: Table S3).

When fitting the general taper model, we took into account the hierarchical structure of the data, which relies on the multiple stem measurements realized along each sample tree. We grouped these within-tree observations ( $l$ ) into upper hierarchy levels: tree ( $k$ ), species ( $j$ ) and site ( $i$ ) (several trees per species and per site). Within-tree observations are likely to be correlated with the correlation as a function of distances between measurements (Tasissa and Burkhart, 1998). This violates the assumption of independence required to apply the nonlinear least squares method, resulting in unbiased parameter estimates but biased and inconsistent estimates of their variance (West et al., 1984). Mixed-effects models allow autocorrelation to be at least partly accounted for by including random effects (Burkhart and Tomé, 2012). The random effects are assumed to follow a multivariate normal distribution with a mean of zero and a positive-definite variance-covariance matrix. Additionally to the mixed – effect approach, the reduction of the correlations among within-tree observations was taken into account with the first order continuous autoregressive structure. The Eq. 2. thus became:

$$D_{area\ ijkl} = \frac{D_{POM\ ij,k} h_{ij,k,l}^{a_{i,j,k}}}{H_{POM\ ij,k}^{a_{i,j,k}}} + \varepsilon_{ijkl} \quad 3.$$

With,

$$a_{i,j,k} = (\beta_1 + b_{1\ i} + b_{1\ ij} + b_{1\ ij,k}) + \beta_2 D_{POM\ ij,k} + \beta_3 h:dc_{ij,k} + \beta_4 h:d^2_{ij,k} + \beta_5 Sp_{i\_X} + \beta_6 D_{convHull130\ ij,k} + \beta_7 Site\_X + \dots + \beta_n X_n \quad 4.$$

$D_{area\ ijkl}$  is a cross-section area at height  $l$  for tree  $k$  belonging to species  $j$  in Site  $i$ ,  $a_{i,j,k}$  is the taper model parameter for tree  $k$  belonging to species  $j$  in Site  $i$ .  $\beta = (\beta_1, \dots, \beta_n)$  are the fixed effects (general parameters),  $b_{1\ i}$  is the site-level random effect,  $b_{1\ ij}$  is the species within site-level random effect and  $b_{1\ ij,k}$  is the tree within the species and site and  $\varepsilon_{ijkl}$  is the within group residual error.  $Sp_{i\_X}$  and  $Site\_X$  are dummy covariates. The random effect  $b_{1\ i}$  is assumed to be independent

for different  $i$ ,  $b_{1ij}$  is assumed to be independent for different  $i, j$  and independent of  $b_{1i}$ ,  $b_{1ij,k}$  is assumed to be independent for different  $i, j, k$  and independent of  $b_{1ij}$  as well as independent of  $b_{1i}$ . The  $\varepsilon_{ijkl}$  are assumed to be independent for different  $i, j, k, l$  and independent of the random effects. The vector of tree random effects and the vector of within-tree residual error terms ( $\varepsilon_l$ ) are both assumed to be multivariate normally distributed (Lejeune et al., 2009). The variance-covariance matrix of the within-tree error terms ( $R_i$ ) was modeled through a first-order autoregressive correlation structure (Eq. 5.) and an exponential function of the variance covariate (Eq. 6.), which provided the best fit.

$$\text{corr}(\varepsilon_{ijkl}, \varepsilon_{ijkl'}) = \rho_{ijkl'} = \rho^{|h_{ijkl} - h_{ijkl'}|} \quad 5.$$

$$\text{Var}(\varepsilon_{ijkl}) = \sigma^2 \exp(2\delta_{S_{ijkl}} v_{ijkl}) \quad 6.$$

Where  $\delta$  is a vector of variance parameters for each level of the stratification variable  $S$  (the species in the study) and  $v_{ijkl}$  is a vector of variance covariates.

We tested the different fixed-effects covariates in the nested models using a stepwise backward approach and we evaluated the significance of a fixed parameter by using conditional t-tests. We compared the models fitted by maximum likelihood with a different number of fixed parameters by means of likelihood ratio tests including, in the final stage, models with the variance function and the autocorrelation structure. All models were also evaluated based on the distribution of the residuals, the RMSE, the RMSE of the cross-sections at 1.3 m only ( $RMSE_{130} = \sqrt{\frac{1}{n_k} \cdot \sum_1^{n_k} (\hat{D}_{area130,k} - D_{area130,k})^2}$ ) and the AIC. In the case of the general taper models (Eq. 3. and 4.), we also included the mean absolute error ( $MAE = \frac{1}{n} \cdot \sum_1^n |\hat{D}_{area l,k} - D_{area l,k}|$ ) as it is less sensitive to large individual errors than RMSE. Relative RMSE and MAE were computed by dividing them with the mean tree diameter  $D_{POM}$  of the dataset. We finally selected the best models based on all covariates and on covariates commonly available in forest inventory data.

## 2.5 Effect of the $H_{POM}$ harmonization

### 2.5.1 Tree-level AGB estimates

In order to assess the relevance of the  $H_{POM}$  harmonization in biomass prediction, we compared the performance of AGB allometric models using as the main predictor, alternatively  $D_{POM}$  (with  $H_{POM} \geq 1.3$  m) or DBH, the harmonized diameter at breast height (i.e.  $D_{POM}$  for trees with  $H_{POM} = 1.3$  m or DBH', the equivalent DBH for trees with  $H_{POM} > 1.3$  m). For this analysis, we used

destructive measurements available for 140 trees (Appendix S1: Table S4) sampled in northern Congo in the frame of the PREREDD+ project (Fayolle et al., 2018) in a site close (18 km) to the second site of the taper study. Note that the basal area was indirectly measured on each stump by photographing the cross-sections of the stump covered with a graduated Plexiglas. The images were then orthorectified and the stump cross-sections were digitized in a GIS software allowing an accurate estimate of the stump area (Bauwens et al., 2017; Bauwens and Fayolle, 2014; Fayolle et al., 2013). For trees with  $H_{\text{POM}}$  higher than the breast height, the equivalent diameter at breast height (DBH') was thus computed by back-transforming the  $\log(\text{DBH}')$  from the linear interpolation of the couple of points  $\log(D_{\text{area\_stump}})$ - $\log(H_{\text{stump}})$  and  $\log(D_{\text{POM}})$ - $\log(H_{\text{POM}})$ . In this destructive biomass dataset, DBH' is thus interpolated and not estimated from a taper model and could then be assumed as a measurement.

Using the destructive biomass dataset, we tested (i) the assumption that using the DBH instead of  $D_{\text{POM}}$  in the pantropical allometric model developed by Chave et al. (2014) reduced the negative bias encountered on large trees, and (ii) compared the quality of local biomass models fits based on  $D_{\text{POM}}$  or DBH.

The pantropical model tested here is the model 4 in Chave et al. (2014),  $m_{\text{PAN}}$  in Table 1. For local biomass models, we used the same functional form fitted on the destructive biomass dataset using either  $D_{\text{POM}}$  (hereafter  $m_{\text{LOC-DPOM}}$ ) or DBH (hereafter  $m_{\text{LOC-DBH}}$ ) as the tree diameter predictor (Table 1).

The relevance of each of AGB estimates from the four approaches (i.e.,  $\text{AGB}_{\text{PAN-DPOM}}$ ,  $\text{AGB}_{\text{PAN-DBH}}$ ,  $\text{AGB}_{\text{LOC-DPOM}}$  and  $\text{AGB}_{\text{LOC-DBH}}$ ) was assessed by the mean error  $\left(\frac{1}{n} \times \sum_{i=1}^n (\widehat{\text{AGB}}_i - \text{AGB}_i)\right)$ , the mean relative error  $\left(\frac{1}{n} \times \sum_{i=1}^n \left(\frac{\widehat{\text{AGB}}_i - \text{AGB}_i}{\text{AGB}_i}\right)\right)$ , and using a t-test to gauge the presence of bias.

The performances of the local AGB models (i.e.,  $m_{\text{LOC-DPOM}}$  and  $m_{\text{LOC-DBH}}$ ) were also assessed with their respective AIC.

## 2.5.2 Plot-level estimates of AGB stock and stock change

Finally, we assessed the impact of the  $H_{\text{POM}}$  harmonization at the 1-ha plot scale using eight permanent sampling plots located in the second site in the north of the Republic of Congo (see Panzou et al., 2018 and Forni et al., 2019 for further details of the site). For this assessment, we

compared the plot AGB estimates from the four approaches: Pan- $D_{\text{POM}}$ , Pan-DBH, Loc- $D_{\text{POM}}$  and Loc-DBH (Table 1). For the two approaches requiring DBH, we first estimated the equivalent DBH (i.e. DBH') of the trees with  $H_{\text{POM}} > 1.3$  m. Then, we estimated the height of each tree in the plots using height:diameter allometry models calibrated on the destructive biomass dataset. Two distinct height:diameter models were fitted and used depending on whether the approach required  $D_{\text{POM}}$  (TH- $D_{\text{POM}}$  model) or DBH (TH-DBH model) as predictor. We then estimated total plot AGB by summing tree-level AGB estimates derived from the four approaches. The plot AGB estimated with the  $m_{\text{LOC-DBH}}$  model was used as the reference, and compared with the three other sets of AGB estimates.

Following the same procedure, we assessed the effect of  $H_{\text{POM}}$  harmonization on plot AGB stock changes using inventory data collected four years after the first census.

### 3 Results

#### 3.1 Variability in the stem profile

We first fitted the taper model (Eq. 2.) to each tree separately and thus obtained one taper parameter  $a_i$  for each of the 228 trees. The values of the taper parameter  $a$  were normally distributed around a mean of  $-0.123 \pm 0.049$  (Appendix S1: Fig. S1). The RMSE of the predicted diameters was 3.8 cm for trees with a  $D_{\text{POM}}$  ranging from 17 cm to 249 cm.

There was a high intraspecific variation in  $a$  for most species (Fig. 3 and Appendix S1: Fig. S2) except Sapelli (*E. cylindricum*), Iroko (*M. excelsa*) and Emien (*A. boonei*). An interspecific variation of  $a$  was also noticed, with Iroko (highest mean value,  $a = -0.062$ ) and Ako (lowest mean value,  $a = -0.180$ ) being the species for which  $a$  deviated the most from the average. A virtual Iroko (resp. Ako) tree with  $D_{\text{POM}} = 100$  cm and  $H_{\text{POM}} = 3.3$  m ( $H_{\text{POM}}$  frequently encountered for these species, see Appendix S1: Table S1), would have a DBH' of 106 cm (resp. 118 cm). Note the average difference between  $D_{\text{POM}}$  and DBH' on the 228 trees is -12 cm.

#### 3.2 Toward a general taper model

After assessing the potential of Eq. 2. to fit the taper of each of the 228 trees with 3D data, we generalized the model by fitting Eq. 3. using all the cross-sections of the 228 trees in one single model. We tested many covariates in Eq. 4. to accommodate for individual variations of the taper parameter  $a_{i,j,k}$ . Among all the fixed covariates tested  $h:d_c$  ( $P = 0.003$ ,  $F = 8.6$ ) and  $h:d^2$  ( $P = 0.0004$ ,  $F = 12.7$ ) were found to be significant and kept in model m1 (RMSE = 6.9 cm, MAE = 3.7 cm, and mean error = -0.9 cm, Table 2). To obtain an operational taper model that can be applied in any forest inventory plot in central Africa, despite their significance we removed some covariates such as  $D_{\text{convHull130}}$  and metrics related to  $D_{\text{convHull130}}$  (e.g.,  $h:d_c$ ), leading to the model m2 with only  $D_{\text{POM}}$  as significant covariate ( $P < 0.001$ ,  $F = 15.2$ , Table 2). The parameters of the selected covariates for m1 and m2 are provided in Table 3. In comparison to the taper model fitted on individual trees (section 3.1, RMSE = 3.8 cm), using a general taper model increased the RMSE by 3.2 to 4 cm depending on the model, resulting in RMSE values of 7 and 7.8 cm for m1 and m2, respectively (Table 2, Fig. 4).

The inclusion of the correlation structure (Eq. 4) in the final step of the model selection removed almost all the correlations (Appendix S1: Fig. S4 and S5). Consequently, the number of significant

covariates was reduced and overfitting avoided. Nevertheless, we additionally tested the site effect at the species level, for the three species having balanced sampling between second and third sites, namely Dabema, Ohia and Padouk (Appendix S1: Fig. S2b). The Student t-test performed on the taper parameter did not reveal any significant site effect for these three species, with respectively  $P = 0.06$  ( $df = 10.2$ ),  $P = 0.4$  ( $df = 18.7$ ), and  $P = 0.8$  ( $df = 9.9$ ). In addition, using nonlinear mixed models fitted for each species separately and including the *Site*,  $h:d_c$  and  $h:d^2$  as covariates provided the same results. We also further investigated the species effect and found that including  $D_{\text{convHull130}}$  (or derived metrics as  $h:d_c$ ) can compensate, in addition to other metrics, the absence of the species covariate and even outperform models including the species factor in terms of RMSE and Bias (results not shown).

The estimated equivalent diameter  $DBH'$  with the models m1 and m2 have a RMSE of 7 cm and 8 cm respectively (Table 2).  $DBH'$  predicted with model m1 do not show any important bias (mean error = -0.9 cm) and, following Piñeiro et al. (2008), the comparison of observed versus predicted  $DBH'$  lead to a coefficient of determination of 0.98 with no significant deviance to the line 1:1 (Table 2 and Appendix S1: Fig. S6 A). The  $DBH'$  predicted with model m2 are, on average, slightly underestimated (mean error = -1.5 cm) and more specifically for very large trees (Table 2, Appendix S1: Fig. S6 B).

### 3.3 Effect of $H_{\text{POM}}$ harmonization on tree-level AGB estimates

Based on the destructive data available for 140 trees, we compared the prediction error associated with the use of  $DBH$  and  $D_{\text{POM}}$  in AGB models following four approaches (Pan- $D_{\text{POM}}$ , Pan- $DBH$ , Loc- $D_{\text{POM}}$  and Loc- $DBH$ , Table 4). The mean prediction error for  $AGB_{\text{PAN-}D_{\text{POM}}}$  estimates was slightly different from zero across all trees sizes (mean = -0.348 Mg,  $P = 0.017$ ) and significantly different from zero for large trees (i.e.,  $D_{\text{POM}} \geq 70$  cm, mean = -1.430 Mg,  $P = 0.009$ , Table 4 and Appendix S1: Fig. S7). The relative error was positive for all the four approaches with a mean relative error of almost 10% for  $AGB_{\text{PAN-}DBH}$ . The unbalanced numbers of trees along the diameter range lead to a positive mean relative error for all the four approaches. Indeed, this positive mean relative error was mostly driven by the high number of trees with  $D_{\text{POM}} < 70$  cm which had an overall systematic positive error (Table 4 and Appendix S1: Fig. S7).

When fitting local AGB models, we found that tree AGB was better predicted by the model  $m_{\text{LOC-}DBH}$  (AIC = -50.4) than by  $m_{\text{LOC-}D_{\text{POM}}}$  (AIC = -37.9) with lower mean errors occurring across all

trees sizes (Table 4 and Appendix S1: Fig. S7). The Akaike weights of these models were respectively 0.002 and 0.998, meaning that the local AGB model fitted with DBH is  $0.998/0.002 = 499$  times more likely to be the best model in terms of Kullback–Leibler discrepancy than the model fitted with  $D_{\text{POM}}$  (Wagenmakers and Farrell, 2004). We thus considered the  $m_{\text{LOC-DBH}}$  model as our reference model in the plot-level analysis. Note that the AIC (and AIC<sub>w</sub>) of TH-DBH and TH- $D_{\text{POM}}$  models are 836 (0.72) and 838 (0.28) respectively. Allometry relationships relating either AGB or TH to the tree diameter show thus better fits with DBH than  $D_{\text{POM}}$ .

### 3.4 Effect of $H_{\text{POM}}$ harmonization on plot-level AGB stock and stock change estimates

First, we used the taper model  $m_2$  to estimate the DBH' of trees with a raised POM in the forest inventory data. Then, we predicted tree AGB with the reference model (i.e.,  $m_{\text{LOC-DBH}}$ ) and summed AGB for all trees within a plot. We found, AGB stocks to equal  $401 \pm 96 \text{ Mg ha}^{-1}$  on average ( $\pm$  sd) and, the annual AGB stock changes to  $6.2 \pm 0.8 \text{ Mg ha}^{-1} \text{ year}^{-1}$  on average ( $\pm$  sd). The average contribution of large trees ( $D_{\text{POM}} \geq 70\text{cm}$ ) to AGB stock and stock changes were  $46 \pm 13 \%$  and  $26 \pm 7 \%$ , respectively. For very large trees ( $D_{\text{POM}} > 140 \text{ cm}$ ), these contributions decreased to  $20 \pm 13 \%$  and  $7 \pm 3 \%$  (Appendix S1: Fig. S8).

Using  $D_{\text{POM}}$  to estimate tree AGB (i.e., Loc- $D_{\text{POM}}$  and Pan- $D_{\text{POM}}$  approaches) led to an underestimation of AGB stocks at the plot level in comparison with the reference approach. The magnitude of this underestimation increased with the proportion of (large) trees with trunk irregularities (Fig. 6A and Appendix S1: Fig. S9 and S10). Depending on the approach used with  $D_{\text{POM}}$ , the underestimation reached -10 to -15% in the plots with the highest abundance of trees with  $H_{\text{POM}}$  superior to 1.3 m height.

The estimates of AGB stock changes obtained when using approaches with  $D_{\text{POM}}$  were not, on average, significantly different from those obtained with the reference approach ( $P = 0.052$  and  $P = 0.745$  for Loc- $D_{\text{POM}}$  and Pan- $D_{\text{POM}}$ , respectively). For some plots, deviations between the two estimates were, however, larger than 5%, and tended to be increasingly negative as the plot basal area contribution of trees with  $H_{\text{POM}}$  superior to 1.3 m height increased (Fig. 5B). This negative deviation disappeared when using DBH (i.e., Pan-DBH, the horizontal orange line in Fig. 5B). However, using Pan-DBH approach led to an average positive deviation of 2.2% ( $P < 0.001$ ) compare to estimates derived from the reference AGB model.

## 4 Discussion

### *The taper of irregularly shaped stems well captured by a simple taper model*

In this study, we developed general taper models having RMSEs ranging from 7 % to 7.8% for trees with different types of stem irregularities (Table 2). These RMSE values are similar to the range of values (4.9% – 8.5%) obtained with species-specific taper models predicting tree diameter of the lower stem part of more regularly-shaped boreal conifers species (Lejeune *et al.* 2009 and, Garber and Maguire, 2003). Here, our dataset mainly combined irregular tree stems from three sites in central Africa, including several species and notably covering a large range of diameters ( $D_{\text{POM}} = 17 \text{ cm} - 249 \text{ cm}$ ). Our results thus suggest that simple taper models can be developed and be yet performant, even on mixes of tropical species with contrasted stem irregularities.

### *An improved AGB allometry when using equivalent diameter at breast height*

We could expect that for trees with irregularities such as buttresses, using an equivalent diameter at breast height would have added noise to the relationship between stem lateral size (diameter, circumference or basal area) and tree AGB. Nevertheless, we found that power AGB models calibrated with DBH (i.e.,  $D_{\text{POM}}$  for trees with regular stems and  $\text{DBH}'$  for irregular stems) was more accurate than the same model using the conventional  $D_{\text{POM}}$  of all the trees, confirming the results obtained by Bauwens *et al.* (2017) for one species. The improvement brought by DBH over  $D_{\text{POM}}$  should be further studied in other sites and forest types as the distribution of the model error versus sampled tree size might not show the same pattern as the one observed in our study (see Fayolle *et al.* 2018 for examples of various AGB error pattern according to sites). Moreover, using DBH to improve the goodness of fit of other types of AGB models than the power model on the product  $\rho \cdot D^2 \cdot \text{TH}$ , should be further studied to ensure that DBH is a reliable predictor for tree AGB estimates of any tropical trees. More complex general allometries with non-power models or power models with more than one entry have been shown to provide better fits (Fayolle *et al.*, 2018; Picard *et al.*, 2015) and could be investigated with DBH.

### *$H_{\text{POM}}$ harmonization to mitigate AGB estimation bias induced by the widely used pantropical AGB model*

Using the equivalent diameter at breast height ( $\text{DBH}'$ ) in the published pantropical AGB model  $m_{\text{PAN}}$  reduced the negative bias on AGB estimates for large irregularly shaped tree stems (Chave *et al.* 2014). The reduction of this ‘allometric bias’ has been earlier demonstrated on a smaller

dataset from Cameroon (Bauwens et al. 2017). At the plot level, using DBH' removed the increasing negative AGB prediction error observed with the increasing abundance of irregular tree stems. By removing this error pattern, the  $H_{POM}$  harmonization renders AGB estimates comparable between plots with different shares of irregular tree stems. However, the harmonization led to a systematic positive deviation of plot-level AGB estimates of about 2% when compared to estimates obtained from our reference AGB model (Fig. 5). This systematic deviation is probably due to the high number of small trees within plots ( $D < 70$  cm), for which the systematic overestimation of AGB is more important when using the pantropical AGB model whatever the type of diameter used (*Pan- $D_{POM}$*  or *Pan-DBH*, see Table 4 and the local maxima in the loess curves in Appendix S1: Fig. S7B). The systematic overestimation of AGB for small trees could be avoided by segmenting the AGB power model (Picard et al., 2015). Therefore, in absence of an AGB model fitted with DBH', using the published pantropical AGB model of Chave et al. (2014) with DBH' is an efficient way to correct for plot-level AGB estimation bias associated with nonstandard  $H_{POM}$ , and the overall small positive bias of 2 % resulting from this estimation approach could be corrected *a posteriori*.

### ***A higher AGB growth for trees with $H_{POM} > 1.3m$ when taking into account the $H_{POM}$ in AGB estimates***

The displacement of the  $H_{POM}$  over time, because of the height growth of the buttresses, adds an additional source of uncertainty on tree growth (Cushman et al., 2014; Muller-Landau et al., 2014, Talbot et al. 2014). Different correction procedures can be used to account for this uncertainty on tree growth estimates and the choice of the appropriate correction procedure depends on the objective of the analysis, in particular, whether it focuses on among-plot or within-plot AGB changes (Cushman et al., 2014; Talbot et al. 2014). Nevertheless, the derivative of the AGB model ( $m_{PAN}$  or  $m_{LOC-DBH}$ ) is higher when considering the equivalent diameter at breast height DBH' for trees with raised POM (see the slopes of the curves from  $m_{LOC-DBH}$  in Appendix S1: Fig. S11). Therefore, tree AGB change between two censuses will be higher when using DBH' than a corrected  $D_{POM}$ , whatever the growth correction procedure. Harmonizing the  $H_{POM}$  would thus limit this growth underestimation. To prevent  $H_{POM}$  changes over time due to the buttress development, an alternative long-term solution would be to set a new standard height that remains above buttresses during the whole ontogeny of individuals belonging to species known to develop buttresses. Following this reasoning, Picard & Gourlet-Fleury (2008) recommended setting the  $H_{POM}$  at a standardized height of 4.5 m for all trees of such species. The development of new AGB models including this higher standard POM height for these species would then be necessary (Muller-Landau et al., 2014).

### ***Reducing uncertainty on plot-level AGB stock change estimates***

At the plot level, AGB stock changes are mainly driven by the small trees (Ligot et al. 2018), and the divergences in AGB stock changes based on our reference model and the pantropical model are mainly coming from trees with  $D_{POM} \leq 70cm$  (Appendix S1: Fig. S9 and S10). The local positive bias for small trees in AGB power model on the product  $\rho \cdot D^2 \cdot TH$  should be further investigated (Picard et al., 2015) in order to reduce as much as possible the AGB stock change uncertainty of small trees. In addition, for AGB stock changes comparison among plots, controlling the  $H_{POM}$  variation is required. Reducing the stock changes uncertainty from the two uncertainty sources described in this section would increase the overall carbon sink of structurally intact tropical forests for example. Note the analysis presented here looks at AGB stock change over a relatively short period (4 years). The difference in AGB stock change estimates with and without harmonizing  $H_{POM}$  may show a different pattern over longer monitoring periods (higher

negative trend or a positive trend) because of the change in  $H_{POM}$  distribution within a plot through time and the higher probability of mortality events including large trees with  $H_{POM} > 1.3\text{m}$ .

### ***Perspectives for improved AGB estimation***

The  $H_{POM}$  distribution within forest inventory plots should be accounted for to avoid any local/regional AGB negative bias associated with spatial variation in the abundance of irregular tree stems.  $H_{POM}$  should thus be measured and reported in forest inventories, but also in destructive AGB datasets (Muller-Landau et al., 2014). For instance, the absence of the  $H_{POM}$  information, or any tree morphological characteristics besides  $D_{POM}$ , TH and  $\rho$ , in the pantropical dataset used by Chave et al. (2014), strongly limits the investigations on the error source.

In this study, we have shown that a simple, multi-specific taper model could be used to mitigate tree-level AGB estimation bias and its propagation to plot level. Since 3D data on tropical trees are becoming more available using TLS technology and the emergence of databases with thousands of trees already scanned and processed across the globe (e.g., Verbeeck et al. 2019), we believe there is an unprecedented opportunity to refine general taper models, or even develop species-specific models for the most important species. Indeed, while tropical forests are hyper-diverse, only a handful ‘hyperdominant’ species constitute the majority of the biomass stock (Bastin et al., 2015). Following the procedure presented here, general or specific taper models could be easily integrated into automatic biomass estimation routines – such as in the BIOMASS R package (Réjou-Méchain et al., 2015) – to correct tree diameters from  $H_{POM}$  variation. The data required for this correction,  $H_{POM}$  and  $D_{POM}$ , is already available in many forest inventories and this correction procedure could thus be performed with no additional burden on AGB model end-users. Furthermore, we could reduce the uncertainty related to  $H_{POM}$  harmonization by measuring, in addition to the  $H_{POM}$  and  $D_{POM}$ , the circumference around the stem irregularities at the reference 1.3 m height (the equivalent to  $D_{convHull130}$  in this study) in forest inventory plots. Indeed, the models having this additional measurement have better performances to estimate DBH’ as demonstrated here and earlier (Ngomanda et al., 2012 and Bauwens et al., 2017).

## **5 Conclusion**

We showed that harmonizing tree diameter measurement height with taper models can reduce biomass underestimation for large trees by allometric models, and this correction can have large (up to 15%) implications for plot-level biomass estimates. Reducing biases in biomass estimates

among tropical forest plots is important to improve our understanding and monitoring of the global carbon budget and has direct implications on the calibration/validation of spaceborne biomass models.

Accepted Article

## **Acknowledgments**

Our thanks go to the Fonds Français pour l'Environnement Mondial (FFEM) and the French Development Agency (AFD), which co-funded the DynAfFor project at the origin of this work (Conventions CZZ 1636.01 D and CZZ 1636.02 E). We thank the Center for International Forestry Research (CIFOR), Resources and Synergies Development (RS&D) and the University of Kisangani (UNIKIS), through the REFORCO project funded by the European Union, for their financial and logistic support in DRC, our thanks go more specifically Prof. Boyemba (UNIKIS), Prof. Ndjele (UNIKIS), Prof. Lomba (UNIKIS) and Dr. Ducenne (RS&D). We thank the DynAfFor team for their logistic support and their assistance in the fieldwork in Congo and the CIB-Olam company, partner of the DynAfFor project, who hosts the PSP of Loundoungou, our thanks go more specifically Mr. Forni (CIRAD) and Mr. Istace (CIB). We thank the Institut de Recherche pour le développement (IRD) and the Alpicam company for their logistic support and their assistance in the fieldwork in Cameroon. Bauwens S. time was partially supported with funds (i) from the DynAfFor Project and, (ii) from the World Bank throughout the PreREDD+ Project. We also thank the NGO Nature + for their administrative support and the PDR research fund *3D-stand* (C-15/50/P5224) that supported the purchase of the laser scanning used in the study.

Authors' contributions: SB, SGF and PL conceived the ideas and designed methodology; SB, PP and JL collected the data; SB, GL and PP analyzed and interpreted the data; SB, AF and PP led the writing of the manuscript. SGF, PL and AF secured funding for the study. All authors contributed critically to the drafts and gave final approval for publication.

## **Supporting Information**

Additional supporting information may be found online at: [link to be added in production]

## **Open Research**

Data are available in the Open Repository and Bibliography (ORBI):

<http://hdl.handle.net/2268/262867>

## References

- Alder, D., Synnott, T.J., 1992. Permanent sample plot techniques for mixed tropical forest, Oxford Forestry Institute. ed, Tropical forestry papers. Oxford.
- Bastin, J.-F., Barbier, N., Réjou-Méchain, M., Fayolle, A., Gourlet-Fleury, S., Maniatis, D., de Haulleville, T., Baya, F., Beeckman, H., Beina, D., others, 2015. Seeing Central African forests through their largest trees. *Scientific reports* 5.
- Bauwens, S., Fayolle, A., 2014. Protocole de collecte des données sur le terrain et au laboratoire nécessaires pour quantifier la biomasse aérienne des arbres et pour l'établissement d'équations allométriques. *Nature+*.
- Bauwens, S., Fayolle, A., Gourlet-Fleury, S., Ndjele, L.M., Mengal, C., Lejeune, P., 2017. Terrestrial photogrammetry: a non-destructive method for modelling irregularly shaped tropical tree trunks. *Methods in Ecology and Evolution* 8, 460–471.
- Brown, S., Gillespie, A.J., Lugo, A.E., 1989. Biomass estimation methods for tropical forests with applications to forest inventory data. *Forest science* 35, 881–902.
- Burkhart, H.E., Tomé, M., 2012. Tree Form and Stem Taper, in: Burkhart, H.E., Tomé, M. (Eds.), *Modeling Forest Trees and Stands*. Springer Netherlands, Dordrecht, pp. 9–41.
- Chave, J., Andalo, C., Brown, S., Cairns, M.A., Chambers, J.Q., Eamus, D., Fölster, H., Fromard, F., Higuchi, N., Kira, T., others, 2005. Tree allometry and improved estimation of carbon stocks and balance in tropical forests. *Oecologia* 145, 87–99.
- Chave, J., Condit, R., Aguilar, S., Hernandez, A., Lao, S., Perez, R., 2004. Error propagation and scaling for tropical forest biomass estimates. *Philosophical Transactions of the Royal Society of London. Series B: Biological Sciences* 359, 409–420.
- Chave, J., Réjou-Méchain, M., Búrquez, A., Chidumayo, E., Colgan, M.S., Delitti, W.B., Duque, A., Eid, T., Fearnside, P.M., Goodman, R.C., 2014. Improved allometric models to estimate the aboveground biomass of tropical trees. *Global change biology*.

Chen, Q., McRoberts, R.E., Wang, C., Radtke, P.J., 2016. Forest aboveground biomass mapping and estimation across multiple spatial scales using model-based inference. *Remote Sensing of Environment* 184, 350–360. <https://doi.org/10.1016/j.rse.2016.07.023>

Clark, D.B., Kellner, J.R., 2012. Tropical forest biomass estimation and the fallacy of misplaced concreteness. *Journal of Vegetation Science* 23, 1191–1196. <https://doi.org/10.1111/j.1654-1103.2012.01471.x>

Cushman, K.C., Muller-Landau, H.C., Condit, R.S., Hubbell, S.P., 2014. Improving estimates of biomass change in buttressed trees using tree taper models. *Methods in Ecology and Evolution*.

Fayolle, A., Doucet, J.-L., Gillet, J.-F., Bourland, N., Lejeune, P., 2013. Tree allometry in Central Africa: testing the validity of pantropical multi-species allometric equations for estimating biomass and carbon stocks. *Forest Ecology and Management* 305, 29–37.

Fayolle, A., Ngomanda, A., Mbasi, M., Barbier, N., Bocko, Y., Boyemba, F., Couteron, P., Fonton, N., Kamdem, N., Katembo, J., Kondaoule, H.J., Loumeto, J., Maïdou, H.M., Mankou, G., Mengui, T., Mofack, G.I., Moundounga, C., Moundounga, Q., Nguimbous, L., Nsue Nchama, N., Obiang, D., Ondo Meye Asue, F., Picard, N., Rossi, V., Senguela, Y.-P., Sonké, B., Viard, L., Yongo, O.D., Zapfack, L., Medjibe, V.P., 2018. A regional allometry for the Congo basin forests based on the largest ever destructive sampling. *Forest Ecology and Management* 430, 228–240. <https://doi.org/10.1016/j.foreco.2018.07.030>

Forni, E., Rossi, V., Gillet, J.-F., Bénédet, F., Cornu, G., Freycon, V., Zombo, I., Mazengué, M., Alberny, E., Mayinga, M., Istace, V., Gourlet-Fleury, S. (2019). Dispositifs permanents de nouvelle génération pour le suivi de la dynamique forestière en Afrique centrale : bilan en République du Congo. *Bois et Forêts des Tropiques*, 341 : 55-70.

Garber, S.M., Maguire, D.A., 2003. Modeling stem taper of three central Oregon species using nonlinear mixed effects models and autoregressive error structures. *Forest Ecology and Management* 179, 507–522.

Gibbs, H.K., Brown, S., Niles, J.O., Foley, J.A., 2007. Monitoring and estimating tropical forest carbon stocks: making REDD a reality. *Environmental Research Letters* 2, 045023.

Gonzalez de Tanago, J., Lau, A., Bartholomeus, H., Herold, M., Avitabile, V., Raumonon, P., Martius, C., Goodman, R.C., Disney, M., Manuri, S., 2018. Estimation of above-ground biomass of large tropical trees with terrestrial LiDAR. *Methods in Ecology and Evolution* 9, 223–234.

Goodman, R.C., Phillips, O.L., Baker, T.R., 2014. The importance of crown dimensions to improve tropical tree biomass estimates. *Ecological Applications* 24, 680–698.

Higuchi, N., dos SANTOS, J., Ribeiro, R.J., Minette, L., Biot, Y., Higuchi, N., dos SANTOS, J., Ribeiro, R.J., Minette, L., Biot, Y., 1998. Biomassa da parte aérea da vegetação da Floresta Tropical úmida de terra-firme da Amazônia Brasileira. *Acta Amazonica* 28, 153–153. <https://doi.org/10.1590/1809-43921998282166>

Lau, A., Calders, K., Bartholomeus, H., Martius, C., Raumonon, P., Herold, M., Vicari, M., Sukhdeo, H., Singh, J., Goodman, R.C., 2019. Tree Biomass Equations from Terrestrial LiDAR: A Case Study in Guyana. *Forests* 10, 527.

Lejeune, G., Ung, C.-H., Fortin, M., Guo, X.J., Lambert, M.-C., Ruel, J.-C., 2009. A simple stem taper model with mixed effects for boreal black spruce. *European journal of forest research* 128, 505–513.

Lutz, J.A., Larson, A.J., Swanson, M.E., Freund, J.A., 2012. Ecological Importance of Large-Diameter Trees in a Temperate Mixed-Conifer Forest. *PLOS ONE* 7, e36131. <https://doi.org/10.1371/journal.pone.0036131>

McRoberts, R.E., 2010. Probability- and model-based approaches to inference for proportion forest using satellite imagery as ancillary data. *Remote Sensing of Environment* 114, 1017–1025. <https://doi.org/10.1016/j.rse.2009.12.013>

McRoberts, R.E., Tomppo, E.O., Næsset, E., 2010. Advances and emerging issues in national forest inventories. *Scandinavian Journal of Forest Research* 25, 368–381. <https://doi.org/10.1080/02827581.2010.496739>

Mitchard, E.T., Feldpausch, T.R., Brienen, R.J., Lopez-Gonzalez, G., Monteagudo, A., Baker, T.R., Lewis, S.L., Lloyd, J., Quesada, C.A., Gloor, M., 2014. Markedly divergent estimates of Amazon forest carbon density from ground plots and satellites. *Global Ecology and Biogeography* 23, 935–946.

- Mitchard, E.T., Saatchi, S.S., Baccini, A., Asner, G.P., Goetz, S.J., Harris, N.L., Brown, S., 2013. Uncertainty in the spatial distribution of tropical forest biomass: a comparison of pan-tropical maps. *Carbon balance and management* 8, 10.
- Molto, Q., Rossi, V., Blanc, L., 2013. Error propagation in biomass estimation in tropical forests. *Methods in Ecology and Evolution* 4, 175–183. <https://doi.org/10.1111/j.2041-210x.2012.00266.x>
- Muller-Landau, H.C., Detto, M., Chisholm, R.A., Hubbell, S.P., Condit, R., 2014. Detecting and projecting changes in forest biomass from plot data. *Forests and Global Change*, Coomes, DA, Burslem, DFRP, Simonsen, WD,(Eds.), Cambridge University Press, Cambridge 381–416.
- Ngomanda, A., Mavouroulou, Q.M., Obiang, N.L.E., Iponga, D.M., Mavoungou, J.-F., Lépengué, N., Picard, N., Mbatchi, B., 2012. Derivation of diameter measurements for buttressed trees, an example from Gabon. *Journal of tropical ecology* 28, 299–302.
- Nogueira, E.M., Fearnside, P.M., Nelson, B.W., Barbosa, R.I., Keizer, E.W.H., 2008. Estimates of forest biomass in the Brazilian Amazon: New allometric equations and adjustments to biomass from wood-volume inventories. *Forest Ecology and Management* 256, 1853–1867. <https://doi.org/10.1016/j.foreco.2008.07.022>
- Overman, J.P.M., Witte, H.J.L., Saldarriaga, J.G., 1994. Evaluation of regression models for above-ground biomass determination in Amazon rainforest. *Journal of Tropical Ecology* 10, 207–218. <https://doi.org/10.1017/S0266467400007859>
- Pan, Y., Birdsey, R.A., Fang, J., Houghton, R., Kauppi, P.E., Kurz, W.A., Phillips, O.L., Shvidenko, A., Lewis, S.L., Canadell, J.G., 2011. A large and persistent carbon sink in the world's forests. *Science* 333, 988–993.
- Panzou, G.J.L., Ligot, G., Gourlet-Fleury, S., Doucet, J.-L., Forni, E., Loumeto, J.-J., Fayolle, A., 2018. Architectural differences associated with functional traits among 45 coexisting tree species in Central Africa. *Functional Ecology* 32, 2583–2593.
- Phillips, O.L., Lewis, S.L., 2014. Evaluating the tropical forest carbon sink. *Global change biology* 20, 2039–2041.

Picard, N. & Gourlet-Fleury, S, 2008. Manuel de référence pour l'installation de dispositifs permanents en forêt de production dans le bassin du Congo. COMIFAC, Yaounde, Cameroon.

Picard, N., Rutishauser, E., Ploton, P., Ngomanda, A., Henry, M., 2015. Should tree biomass allometry be restricted to power models? *Forest Ecology and Management* 353, 156–163. <https://doi.org/10.1016/j.foreco.2015.05.035>

Piñeiro, G., Perelman, S., Guerschman, J. P., & Paruelo, J. M. (2008). How to evaluate models: observed vs. predicted or predicted vs. observed?. *Ecological Modelling*, 216(3-4), 316-322.

Pinheiro, J., Bates, D., 2006. Mixed-effects models in S and S-PLUS. Springer Science & Business Media.

Pinheiro, J., Bates, D., DebRoy, S., Sarkar, D., Team, R.C., 2012. nlme: Linear and nonlinear mixed effects models. R package version 3.

Ploton, P. et al. Aggregated CoFor forest management inventories. figshare (2020) doi:10.6084/m9.figshare.11993541.

Ploton, P., Barbier, N., Momo, S.T., Réjou-Méchain, M., Bosela, F.B., Chuyong, G., Dauby, G., Droissart, V., Fayolle, A., Goodman, R.C., 2016. Closing a gap in tropical forest biomass estimation: taking crown mass variation into account in pantropical allometries. *Biogeosciences* 13, 1571–1585.

Réjou-Méchain, M., Tanguy, A., Piponiot, C., Chave, J., & Hérault, B. (2017). biomass: An R package for estimating above-ground biomass and its uncertainty in tropical forests. *Methods in Ecology and Evolution*, 8(9), 1163-1167.

Slik, J.W., Paoli, G., McGuire, K., Amaral, I., Barroso, J., Bastian, M., Blanc, L., Bongers, F., Boundja, P., Clark, C., 2013. Large trees drive forest aboveground biomass variation in moist lowland forests across the tropics. *Global ecology and biogeography* 22, 1261–1271.

Tasissa, G., Burkhardt, H.E., 1998. An application of mixed effects analysis to modeling thinning effects on stem profile of loblolly pine. *Forest ecology and management* 103, 87–101.

Verbeeck, H., Bauters, M., Disney, M., & Calders, K., 2019. Time for a plant structural economics spectrum. *Frontiers in Forests and Global Change*, 2, 43.

Accepted Article

Wagenmakers, E.-J., Farrell, S., 2004. AIC model selection using Akaike weights. *Psychonomic Bulletin & Review* 11, 192–196. <https://doi.org/10.3758/BF03206482>

West, P.W., Ratkowsky, D.A., Davis, A.W., 1984. Problems of hypothesis testing of regressions with multiple measurements from individual sampling units. *Forest Ecology and Management* 7, 207–224.

Zhao, F., Guo, Q., Kelly, M., 2012. Allometric equation choice impacts lidar-based forest biomass estimates: A case study from the Sierra National Forest, CA. *Agricultural and Forest Meteorology* 165, 64–72. <https://doi.org/10.1016/j.agrformet.2012.05.019>

## Tables

Table 1: AGB models retrieved from the literature ( $m_{PAN}$ ) or fitted in this study ( $m_{LOC-DPOM}$  and  $m_{LOC-DBH}$ ). Model predictors are the basic wood density ( $\rho$ , in  $g\ cm^{-3}$ ), the total height of the tree ( $TH$ , in m) and, the reference stem diameter measured at 1.3 m or above any deformation ( $D_{POM}$ , in cm) or the diameter at breast height ( $DBH$ , in cm) which includes a mix of  $D_{POM}$  for trees measured at 1.3m height and the equivalent diameter at breast height ( $DBH'$ , in cm) for diameter  $D_{POM}$  measured above any deformation ( $H_{POM} > 1.3m$ ).

AGB model	Approach	Equation
$m_{PAN}$	Pan- $D_{POM}$	$AGB_{PAN-DPOM} = 0.673 \cdot (\rho \cdot D_{POM}^2 \cdot TH)^{0.976}$
	Pan- $DBH$	$AGB_{PAN-DBH} = 0.673 \cdot (\rho \cdot DBH^2 \cdot TH)^{0.976}$
$m_{LOC-DPOM}$	Loc- $D_{POM}$	$AGB_{LOC-DPOM} = 0.043 \cdot (\rho \cdot D_{POM}^2 \cdot TH)^{1.018}$
$m_{LOC-DBH}$	Loc- $DBH$	$AGB_{LOC-DBH} = 0.049 \cdot (\rho \cdot DBH^2 \cdot TH)^{1.001}$

Table 2: Goodness of fits of the general taper models (Eq. 2) with different fixed covariates used to predict the taper parameter  $a_{i,j,k}$ . The root mean square error (RMSE), the mean absolute error (MAE) and the mean error were computed over all the cross-sections as well as for cross-sections at a 1.3 m height only. The model  $m1$  requires  $h:d_c$  covariate which is based on  $D_{convHull130}$ , a variable not routinely measured in forest inventory. For model  $m2$ , before the selection of the significant covariates in the fitting process, we only selected covariates that are based on conventional measurements in forest inventories.

Models	Fixed covariates	RMSE (cm)		MAE (cm)		Mean error (cm)		df
		All	1.3	All	1.3	All	1.3	
$m1$	$a \sim h:d_c + h:d^2$	<b>7.0</b> (7.0%)	<b>7.0</b> (7.6%)	<b>3.7</b> (3.7%)	<b>4.2</b> (4.5%)	<b>-0.9</b> (-0.9%)	<b>-0.9</b> (-0.9%)	21
$m2$	$a \sim D_{POM}$	7.8 (7.8%)	8.0 (8.7%)	4.0 (4.0%)	4.7 (5.1%)	-1.5 (-1.5%)	-1.5 (-1.6%)	20

Table 3: General fixed parameters for the two general taper models of the table 2. The parameters correspond to the equation  $a_{ijk} = (\beta_1 + b_{1,i} + b_{1,i,j} + b_{1,i,j,k}) + \beta_2 \cdot D_{POM} + \beta_3 \cdot h:d_c + \beta_4 \cdot h:d^2$  (Eq. 3).

Parameter	Covariate	m1	m2
$\beta_1$	(Intercept)	-0.129	-0.156
$\beta_2$	$D_{POM}$		0.048
$\beta_3$	$h:d_c$	0.014	
$\beta_4$	$h:d^2$	-0.004	

Table 4: Prediction error of the four approaches tested to tree-level AGB estimates with destructive AGB measurements available for 140 trees. The significance of a bias in the mean error was assessed with t-test (\*\*\*) for  $P < 0.001$ , \*\* for  $P < 0.01$ , \* for  $P < 0.05$ , and *ns* for not significant). MAE is the mean absolute error.

AGB prediction approach	Mean error (Mg)		Mean rel. error (%)		MAE (Mg)	
	All sizes	$D_{\text{POM}} \geq 70 \text{ cm}$	All sizes	$D_{\text{POM}} \geq 70 \text{ cm}$	All sizes	$D_{\text{POM}} \geq 70 \text{ cm}$
PAN- $D_{\text{POM}}$	-0.35*	<b>-1.430**</b>	<b>6.2**</b>	-5.7 <sup>ns</sup>	0.87	2.56
PAN-DBH	0.016 <sup>ns</sup>	-0.120 <sup>ns</sup>	<b>9.8***</b>	3.0 <sup>ns</sup>	0.83	2.41
LOC- $D_{\text{POM}}$	0.074 <sup>ns</sup>	0.250 <sup>ns</sup>	4.4*	1.3 <sup>ns</sup>	0.85	2.49
LOC-DBH	0.019 <sup>ns</sup>	0.111 <sup>ns</sup>	4.0*	3 <sup>ns</sup>	0.82	2.41

## Figures

Figure 1: Conventional (left) and original (right) workflows for plot-level aboveground biomass (AGB) stock and stock change estimates. In the original workflow, the height ( $H_{POM}$ ) of the measured  $D_{POM}$  is harmonized at the breast height (i.e., 1.3m) and the resulting equivalent diameter at breast height ( $DBH'$ ) is computed with a taper model before estimating tree AGB of the trees with irregular stems in the forest inventory plots. The taper model and the AGB model used in this study are based on 3D data and destructive data, respectively. In the original workflow, the AGB model has DBH as one of its predictors (i.e.,  $D_{POM}$  for regular stems and  $DBH'$  for irregular ones). The performances of the AGB model from the original workflow are tested in this study and the plot-level AGB stock and stock change estimates of the two workflows are compared.

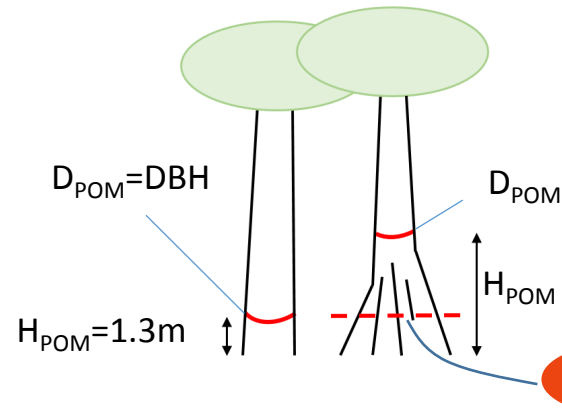
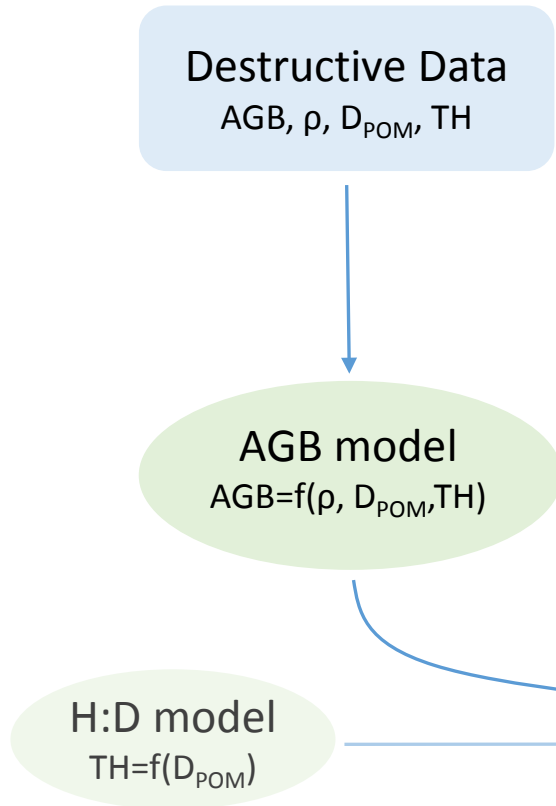
Figure 2: Main attributes used in the taper models. The cross section extracted from the 3D data at the standard breast height (1.3 m) is indicated with all the types of measurements used in the study.

Figure 3: Taper parameter  $a$  of each taper model fitted at the tree-level (Eq. 1) and grouped by species. Solid and dotted vertical red lines represent the mean and the mean  $\pm$  sd of  $a$  across all species, respectively.

Figure 4: Equivalent diameters  $D_{area,i}$  along the stem.  $D_{area,i}$  is predicted from (i) the taper models fitted on each tree separately (green curves) and (ii) the general model  $m1$  fitted on all trees (orange curves). Curves represent  $D_{area,i}$  predictions from the two approaches for five individual trees from species showing contrasted stem shapes. Ayous (*Triplochiton scleroxylon*) and Fromager (*Ceiba pentandra*) are species with well-developed buttresses. Sapelli (*Entandrophragma cylindricum*) is known to develop irregularities at the base of the stem with sometimes buttresses. Emien (*Alstonia boonei*) is a fluted species and Iroko (*Milicia excelsa*) has a more circular stem with some irregularities at the base of the stem for the largest individuals. On the right, the cross-sections of the five trees for two reference heights: the breast height (1.3 m) and the height of the point of measurement ( $H_{POM}$ ) of the reference diameter ( $D_{POM}$ ) located 50 cm above the irregularities. The sizes of the cross-sections are proportional within trees but not among trees.

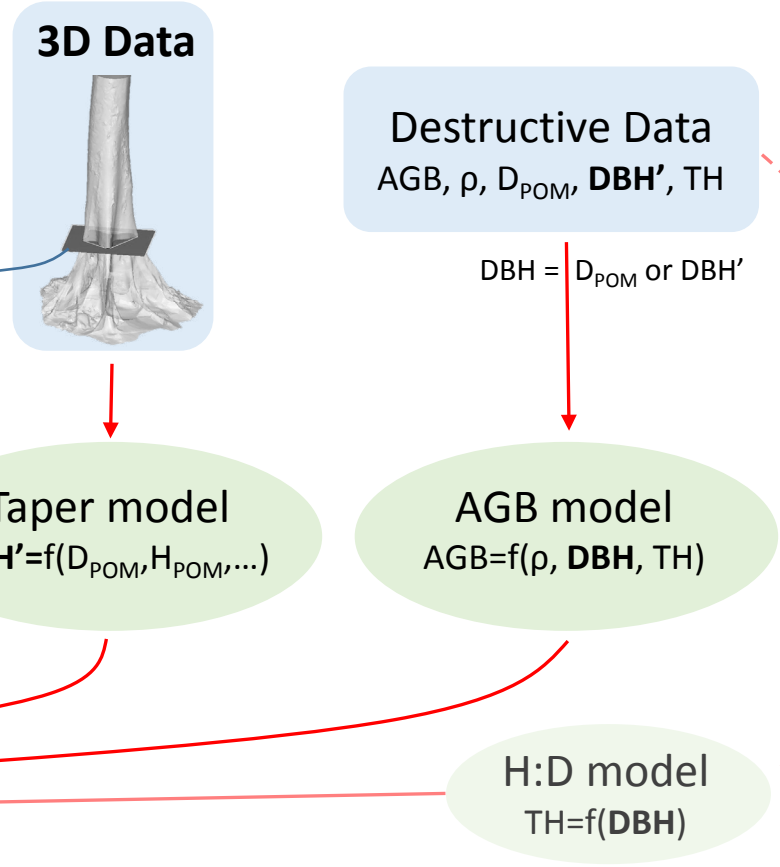
Figure 5: The 1ha plot scale relative difference on AGB stock and stock change between the reference approach Loc-DBH and approaches using  $D_{POM}$  (Loc- $D_{POM}$  and Pan- $D_{POM}$ ) or the pantropical approach with DBH (Pan-DBH). The basal area was computed with DBH. The stock change estimates are based on a 4 years interval re-measurement.

### Conventional workflow



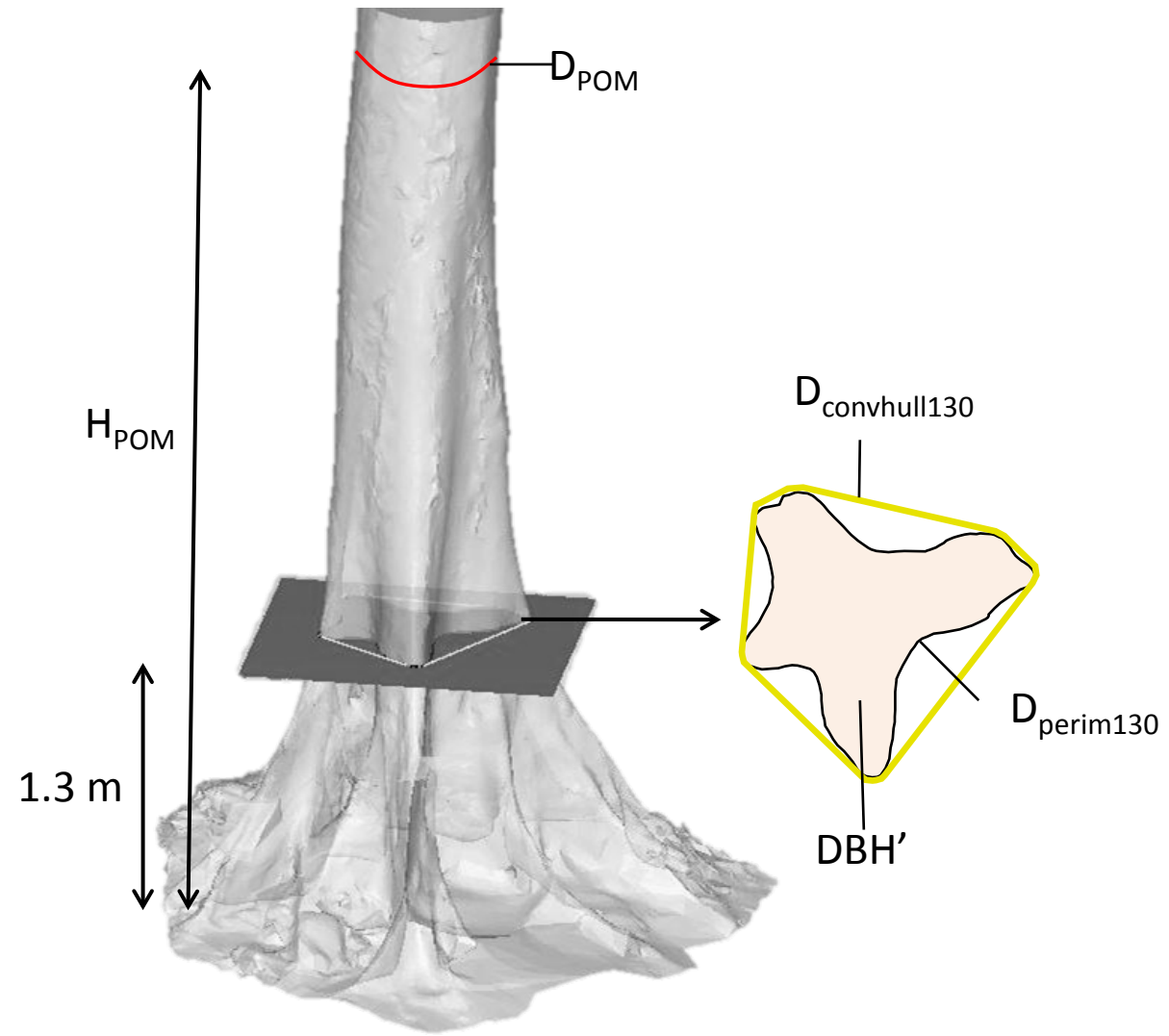
**Plot tree attributes**  
Species,  $D_{POM}$ ,  $H_{POM}$ , (TH), ...

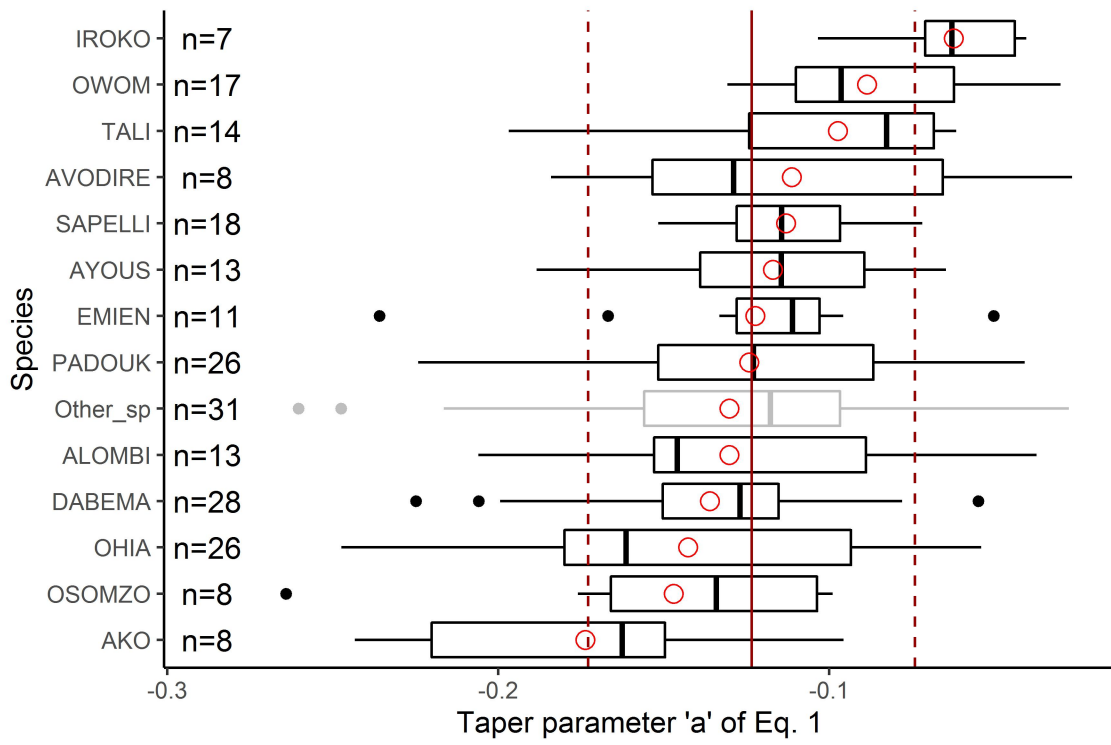
### Original workflow of the study



**Tree-level AGB of the plots**

$\Sigma$   
**Plot-level AGB**  
 $t_1$   
 $t_2$





eap\_2451\_f3.jpeg

